FULL PAPER

BJC

British Journal of Cancer (2016) 115, 203–211 | doi: 10.1038/bjc.2016.190

Keywords: FAK; Y15; Bcl-2; JNK; non-small cell lung cancer

Efficacy of focal adhesion kinase inhibition in non-small cell lung cancer with oncogenically activated MAPK pathways

Hao Zhang[1,4], Huanjie Shao[2,4], Vita M Golubovskaya[3], Hongbin Chen[1], William Cance[3], Alex A Adjei[1] and Grace K Dy[*,1]

[1]Department of Medicine, Roswell Park Cancer Institute, Buffalo, NY 14263, USA; [2]Department of Cell and Developmental Biology, College of Life Sciences, Shaanxi Normal University, Shaanxi 710119, China and [3]Department of Surgical Oncology, Roswell Park Cancer Institute, Buffalo, NY 14263, USA

Background: Focal adhesion kinase (FAK) is overexpressed in many types of tumours, including lung cancer. Y15, a small molecule which inhibits Y397 FAK autophosphorylation, decreases growth of human neuroblastoma, breast and pancreatic cancers. In this study, we investigated the *in vitro* and *in vivo* effects of Y15, and the underlying mechanism on non-small cell lung cancer cells.

Methods: The cytotoxic effects of Y15 targeting FAK signalling were evaluated. Gene-knockdown experiments were performed to determine the anti-cancer mechanism. Xenografts with RAS or EGFR mutations were selected for *in vivo* Y15 treatment.

Results: Y15 blocked autophosphorylation of FAK in a time- and dose-dependent manner. It caused dose-dependent decrease of lung cancer cell viability and clonogenicity. Y15 inhibited tumour growth of RAS-mutant (A549 with KRAS mutation and H1299 with NRAS mutation), as well as epidermal growth factor receptor (EGFR) mutant (H1650 and H1975) lung cancer xenografts. JNK activation is a mechanism underlying Y15-induced Bcl-2 and Mcl-1 downregulation. Moreover, knockdown of Bcl-2 or Bcl-xL potentiated the effects of Y15. The combination of various inhibitors of the Bcl-2 family of proteins with FAK inhibitors demonstrated synergy in multiple lung cancer cell lines *in vitro*.

Conclusions: FAK inhibition demonstrated efficacy both *in vitro* and *in vivo* in lung cancers with either oncogenic RAS or EGFR mutations. In addition, FAK inhibition in combination with inhibitors of Bcl-2 family of anti-apoptotic proteins has synergistic activity in these MAPK-activated non-small cell lung cancer cell line models.

One of the vital hallmarks of cancer which distinguishes it from benign tumours is its capability for tissue invasion and distant metastasis (Lazebnik, 2010). Focal adhesion kinase (FAK) is a non-receptor protein tyrosine kinase identified as a critical signalling molecule mediating host–tumour interactions that affect cell adhesion, invasion, angiogenesis and metastasis via its cross-linked processes with Src-, integrin- and growth factor receptor signalling pathways (Mitra *et al*, 2005; Siesser and Hanks, 2006). FAK is overexpressed in various malignancies, including lung cancer, wherein associated FAK gene amplification portends a worse prognosis (Agochiya *et al*, 1999; Carelli *et al*, 2006). Indeed, FAK activation has been implicated in conferring a more invasive phenotype to malignancies through its effects on the epithelial-to-mesenchymal transition process by promoting E-cadherin delocalisation and upregulation of caveolin-1 (Bailey and Liu, 2008; Cicchini *et al*, 2008).

Y15 is a small molecule identified through *in silico* screening that selectively targets the Y397 autophosphorylation site of FAK

*Correspondence: Dr GK Dy; E-mail: grace.dy@roswellpark.org
[4]These authors contributed equally to this work.

Received 15 January 2016; revised 29 April 2016; accepted 11 May 2016; published online 23 June 2016

(Golubovskaya *et al*, 2008). This is the same interaction site between activated FAK and Src, as well as the binding site for other signalling proteins (Schlaepfer *et al*, 1994; Cary *et al*, 1996). Y15 has shown activity, either alone or in combination with chemotherapy, both *in vitro* and *in vivo*, against breast, pancreatic, neuroblastoma and colon cancer tumour growth (Golubovskaya *et al*, 2008; Hochwald *et al*, 2009; Beierle *et al*, 2010; Heffler *et al*, 2010, 2011).

The FAK-Src signalling network appears to be deregulated in high-grade lung cancers. Phosphoproteomic analysis comparing KRAS-mutant/LKB1 wild-type lung tumours with KRAS-mutant/LKB1-deficient lung tumours revealed hyperphosphorylation of FAK and Src which promoted cell migration in the latter (Carretero *et al*, 2010). This may provide mechanistic explanation for the observation that inactivation of the tumour suppressor LKB1 results in greater propensity for metastasis compared with loss of other tumour suppressors in a KRAS-driven murine lung cancer model (Chen *et al*, 2012). We thus sought to characterise the effects of FAK inhibition using Y15 and other FAK inhibitors in various lung cancer cell lines with or without RAS mutations.

MATERIALS AND METHODS

Cell lines. KRAS-mutant (H157, H358, H727, A549), NRAS-mutant (H1299) and EGFR-mutant (H1650, H1975) cell lines were obtained from the American Type Culture Collection. Cell lines were cultured in RPMI-1640 (Life Technologies, Grand Island, NY, USA) supplemented with 10% FBS (Sigma-Aldrich, St Louis, MO, USA) and penicillin–streptomycin and incubated at 37 °C in a fully humidified atmosphere containing 5% CO_2. All cell lines were used at low passage in our laboratory, and were authenticated using viability, morphology and growth curve analysis on a regular basis, and tested negative for Mycoplasma.

Compounds. Y15 and the ATP-competitive FAK inhibitor PF-573228 were purchased from Sigma-Aldrich. Other ATP-competitive FAK inhibitors PF-562271 and NVP-TAE226 (TAE-226), as well as Bcl-2 inhibitors ABT263, GX15-070 and ABT-737 were obtained from Selleckchem (Houston, TX, USA). FAK inhibitor C4 (Kurenova *et al*, 2009) was obtained from the laboratory of Dr Elena Kurenova and was used as control in the MTS assays to screen for the effect of Y15 on lung cancer cell viability.

Antibodies. The antibodies of p-FAK (Y397), FAK, p-Akt (S473), Akt, p-Erk1/2 (T202/Y204), Erk, p-Src (Y416), Src, cleaved caspase-3, cleaved poly (ADP-ribose) polymerase (PARP), p-STAT3 (Y705), p-P70S6K (T389), p-mTOR (S2448), Bcl-2, Bcl-xL and Mcl-1 were obtained from Cell Signaling Technology (Danvers, MA, USA). p-JNK (T183) and JNK1 antibodies were from Santa Cruz Biotechnology (Dallas, TX, USA). β-Actin antibody was purchased from Sigma-Aldrich.

Clonogenicity assays. In all, 5×10^5 cells were seeded into 6-well plates and treated with escalating dosages of Y15 (or DMSO) and incubated at 37 °C for 14–20 days. Media were changed every 3–4 days. Colonies were then visualised and counted after staining with crystal violet.

Cell-viability assays. Initial screening of Y15 effect on lung cancer cell line viability was performed using trypan blue exclusion assay as previously described (Zhang *et al*, 2014) using C4 as comparator agent. MTS assay was used for all subsequent experiments. Briefly, cells of 1×10^4 were seeded in 96-well plates and treated with concurrent administration of Y15 with each of the drugs for 48 or 96 h. Then 20 μl per well of CellTiter 96 AQueous One Solution Reagent (Promega, Madison, WI, USA) was added. After 1 h at 37 °C in a humidified, 5% CO2 atmosphere, the absorbance at 490 nm was recorded using a microplate reader.

Western blot analysis. For immunoblot analysis, the cells were treated with the indicated agents and then collected in cell lysis buffer (Cell Signaling Technology). Total protein was quantified using Coomassie protein assay reagent (Bio-Rad, Hercules, CA, USA). An equal amount of protein (60 μg) was separated by SDS-PAGE and electrotransferred onto nitrocellulose membrane. The primary antibodies were then tested. β-Actin was used as endogenous control for equal loading. Immunocomplexes were visualised with enhanced chemiluminescence detection kits (Pierce, Rockford, IL, USA).

RNA interference studies. RNA interference was based on pGreenPuro system (System Bioscience, Mountain View, CA, USA) expressing small-hairpin RNA (shRNA). pGreen-Akt1, pGreen-Bcl-2, pGreen-Bcl-xL and pGreenPuro-vec constructs, encoding shRNA for Akt1 (shAkt1), Bcl-2 (shBcl-2), Bcl-xL (shBcl-xL) or a negative control (vector), respectively, were prepared by inserting the target sequence for human Akt1 (5′-ATGACTTCCTTCTTGAGGATC-3′) or Bcl-2 (5′-CCCTGA TTGTGTATATTCA-3′) or Bcl-xL (5′-CCCTTGCAGCTAGTT TTCT-3′) into pGreenPuro. 293TN cell was stably transfected with the constructs and three packaging plasmids using Lipofectamine 2000 reagent (Invitrogen, Carlsbad, CA, USA) to package lentivirus; and then lung cancer cells were infected with lentivirus with multiplicity of infection of 5. Clones with stable down-regulated Akt1, Bcl-2 or Bcl-xL expression were selected with puromycin (1 μg ml^{-1}).

Small-interfering RNA (siRNA) targeting JNK (MAPK8 Silencer Select siRNA S11154) were purchased from Life Technologies. Transient transfection of siRNAs was carried out using Lipofectamine 2000 (Life Technologies) according to the manufacturer's instructions. Briefly, cells were seeded in 24-well plate. On the second day, cells were transfected with 20 pMol siRNA per well with lipofectamine 2000 (Invitrogen), and media were changed 4 h after transfection. Twenty-four hours later, cells were then treated with Y15 for cell-viability analysis.

***In vivo* xenograft experiments.** All *in vivo* experimental protocols were approved by the Institutional Animal Care and Use Committee of Roswell Park Cancer Institute (RPCI; Buffalo, NY, USA). Female SCID mice, 6–8-week old, were used for the experiments. Lung cancer cells (5×10^6) were injected s.c. into the flank of SCID mice (RPCI). Tumours were monitored until they reached a mean tumour volume of 100 or 250 mm^3 before starting Y15 dosing. Mice were assigned randomly to different groups (five mice per treatment group).Y15 was administered by oral gavage once daily at respective doses shown in the accompanying figures (see the 'Results' section). Tumour volume was measured in two dimensions (length and width) twice-weekly using Ultra Cal-IV calipers (Fred V. Fowler Company, Inc., Newton, MA, USA) and was analysed using studylog software (Studylog Systems, San Francisco, CA, USA). Tumour volume (mm^3) = (length × width^2)/2. Mouse body weights were also recorded twice-weekly and the mice were observed daily. Mice with tumour volumes $\geqslant$2000 mm^3 or with losses in body weight $\geqslant$20% from their initial body weight were promptly killed per Institutional Animal Care and Use Committee guidelines.

Immunohistochemistry. Immunohistochemistry was performed in Pathology department of RPCI as previously described (Shao *et al*, 2012). Briefly, tumour tissue was fixed overnight in 10% neutral-buffered formalin at room temperature, transferred to 70% ethanol and processed for paraffin embedding using a Thermo Electron Excelsior tissue processor (Thermo Fisher Scientific, Pittsburgh, PA, USA). Paraffin blocks were sectioned to 4-mm thickness and placed on positively charged glass slides. Tissues were stained using a Discovery automated slide machine (Ventana Medical Systems, Tucson, AZ, USA). Sections were counter-stained with hematoxylin

to enhance visualisation of tissue morphology. After treatment in terminating buffer (300 mM sodium chloride and 30 mM sodium citrate), the sections were incubated in streptavidin–peroxidase complex for 30 min and then developed with diaminobenzidine-tetra-hydrochloride for 1–5 min as a substrate.

Statistical analysis. The reported values represent the means ± s.d. for at least three independent experiments performed in triplicate. To determine the significance between the tested groups, Student's test was used, with $P<0.05$ considered as significant. Median dose–effect analysis was performed using CalcuSyn software version 2 (Biosoft, Great Shelford, Cambridge, UK) to determine additive, synergistic or antagonistic interactions of drug combinations.

RESULTS

Y15 decreases lung cancer cell viability and clonogenicity *in vitro* in a dose-dependent manner. To characterise the effect of FAK inhibition using Y15 in various lung cancer cell lines, the basal expression levels of Y397-pFAK and total FAK in several lung cancer cell lines were analysed (Figure 1A). Levels of Y397-pFAK and FAK were variable across cell lines. We then screened for the efficacy of Y15 against five cell lines with 3-day exposure to escalating doses of Y15. Results showed decreased cell viability by MTS assay, whereas the control agent C4, a FAK scaffold inhibitor which disrupts FAK-VEGFR3 signalling and is not anticipated to be cytotoxic in lung cancer cell lines, had virtually no effect (Figure 1B). MTS assay was also performed for the ATP-competitive small molecule FAK inhibitors PF-562271, PF-573228 and TAE-226. Table 1 demonstrates comparative IC50 values as determined by MTS assay, showing that Y15 is more potent compared with the most selective FAK inhibitor PF-573228, with comparable to slightly more potent activity compared with PF-573228 and TAE-226 (Table 1). We also treated lung cancer cell lines for 72 h and determined IC50 values for Y15 by clonogenic assay (Figure 1C). Y15 decreased clonogenicity in a dose-dependent manner in multiple cell lines regardless of RAS mutation status (Figure 1C).

Y15 effectively inhibits the growth of lung cancer xenografts *in vivo*. To test the efficacy of Y15 on RAS-mutant lung cancer growth *in vivo*, we implanted A549 cells subcutaneously into mice. As shown in Figure 2A, Y15 significantly decreased tumour growth. The same effect was observed with H1299 xenograft

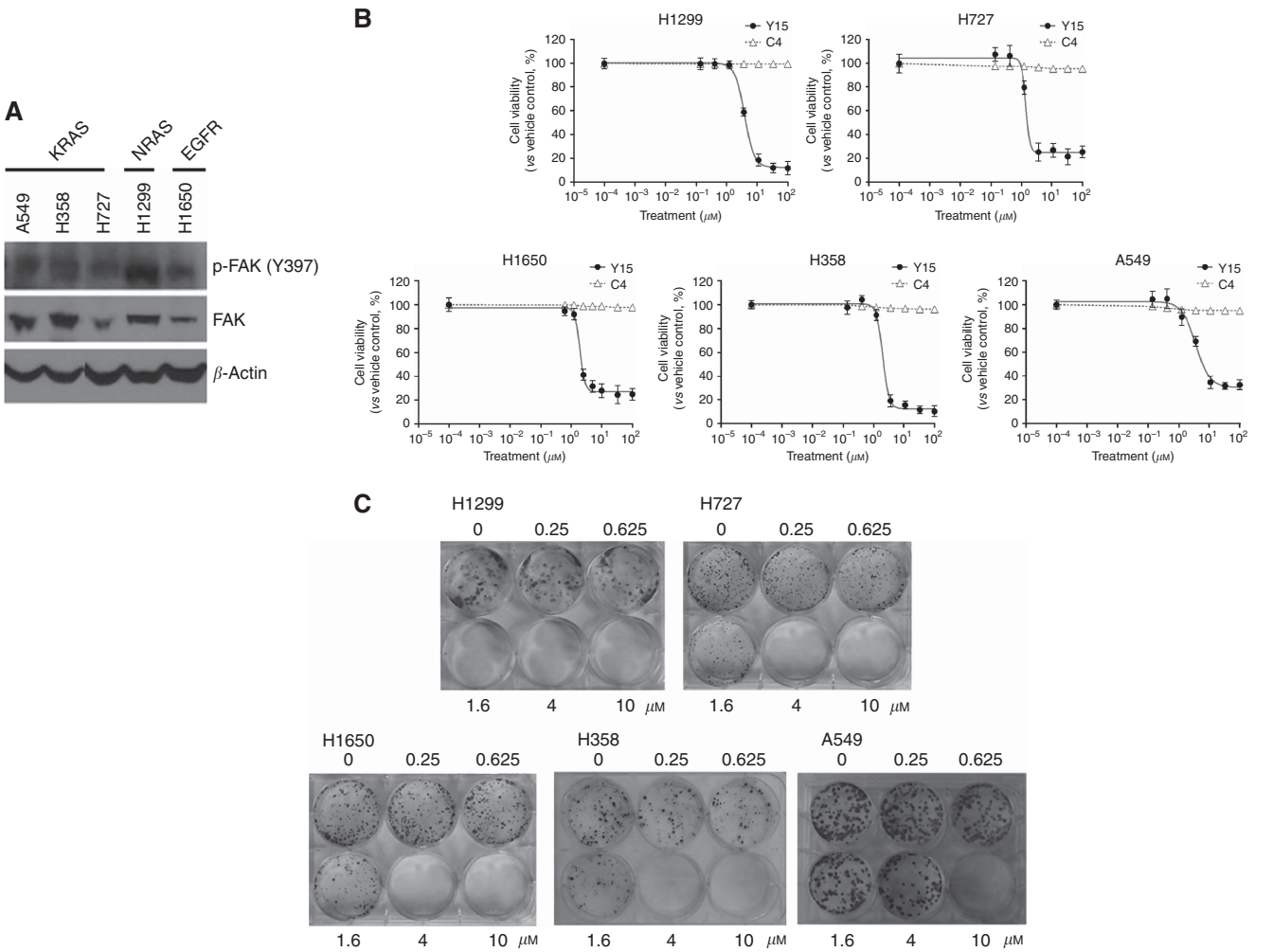

Figure 1. Y15 decreased viability and clonogenicity of lung cancer cell lines in a dose-dependent manner. (**A**) Expression of Y397-pFAK and FAK in lung cancer cell lines. Western blotting with Y397-pFAK and FAK was performed on different lung cancer cell lines. β-Actin was used as a loading control. Y397-pFAK and FAK levels are variable across different cell lines. (**B**) MTS assay. RAS-mutant (H1299, H727, H358, A549) or EGFR-mutant (H1650) cell lines were treated with Y15 or control FAK inhibitor C4 (not targeting Y397-pFAK) for 72 h. Y15 increased cell death in all cell lines, whereas control C4 did not. (**C**) Different lung cancer cells were treated with increasing doses of Y15 for 2 weeks and clonogenicity assay was performed. Y15 significantly decreased clonogenicity in a dose-dependent manner.

(Figure 2B). Immunohistochemical staining demonstrated that Y15 decreased Y397 FAK phosphorylation and triggered activation of caspase-3 in the harvested A549 tumour xenografts compared with the PBS-treated group (Figure 2C). We observed similar growth inhibition in EGFR-mutant H1650 and H1975 xenografts (Figure 2D and E). There was no significant difference in body weights (data not shown) and side effects between the vehicle and Y15-treated animals even when the dosages evaluated. Thus, Y15 can inhibit the growth of lung cancers with oncogenically driven MAPK pathway activation through either RAS or EGFR mutation.

Y15 inhibits Y397 FAK autophosphorylation and downregulates Bcl-2, Bcl-xL and Mcl-1 in a time-dependent manner in non-small cell lung cancer cell lines. To determine the time-dependent effect of Y15 on FAK autophosphorylation, we performed Western blotting on cell lysates at different time points from 0.5 through 72 h exposure to Y15 at 5 μM concentration in the H1299 cells (IC50 $\sim$ 4 μM). Figure 3A shows time-dependent reduction in Y397-pFAK level. We also detected immediate and sustained reduction of phosphorylation of downstream substrate of FAK: p-Src (Y416). There was decreased phosphorylation of Akt, STAT3, P70S6K, GSK3β and mTOR at 72 h as well. There was also evidence of pro-apoptotic effects with decrease in Bcl-2, Bcl-xL and Mcl-1 levels. Intriguingly, phosphorylation of JNK was significantly increased until the 24-h time point, wherein cleavage of PARP and caspase-3 began to increase. However, Erk1/2 (T202/Y204) phosphorylation was not affected. Indeed, reduction of ERK phosphorylation with Y15 treatment was cell line-dependent (data not shown). Similar results were observed in additional cell lines (Figure 3B). Activation of JNK was induced upon treatment of Y15 until 8-h time point, whereas Bcl-2, Bcl-xL and Mcl-1 were decreased with increasing drug exposure time course. In summary, Y15 caused time-dependent decrease of Y397-pFAK, Bcl-2, Bcl-xL and Mcl-1 across multiple cell lines.

Table 1. The effect of Y15 and other FAK inhibitors on lung cancer cell line viability (MTS assay)

Cell line	H157	H358	H727	H1299	A549	H1650	H1975
IC50 (μM)							
TAE226	7.46	3.18	0.30	2.98	2.59	2.30	2.88
PF-562271	5.76	6.38	2.26	3.94	5.41	5.31	5.47
PF-573228	11.39	27.49	2.80	9.18	9.08	20.70	13.20
Y15	2.10	2.72	1.30	3.88	3.49	1.90	1.56

Y15-induced downregulation of Bcl-2 family members is independent of caspase activation. Given that caspase activation induced protein degradation during cell apoptosis, we evaluated whether caspase was involved in the downregulation of Bcl-2 family members. H1299 cells treated with 5 μM Y15 were cultured in the presence or absence of 20 μM pan-caspase inhibitor, z-VAD-fmk, for 8–48 h. As shown in Figure 3C, reduction in both Bcl-2 and Bcl-xL was evident from 8 h onwards under Y15 treatment alone as expected. However, no significant difference in this effect was found with the addition of caspase inhibitor z-VAD. Similar result was found in Mcl-1 from 24–48 h treatment. Taken together, the above results showed that downregulation of Bcl-2 family members accompanying Y15-induced apoptosis was independent of caspase activation.

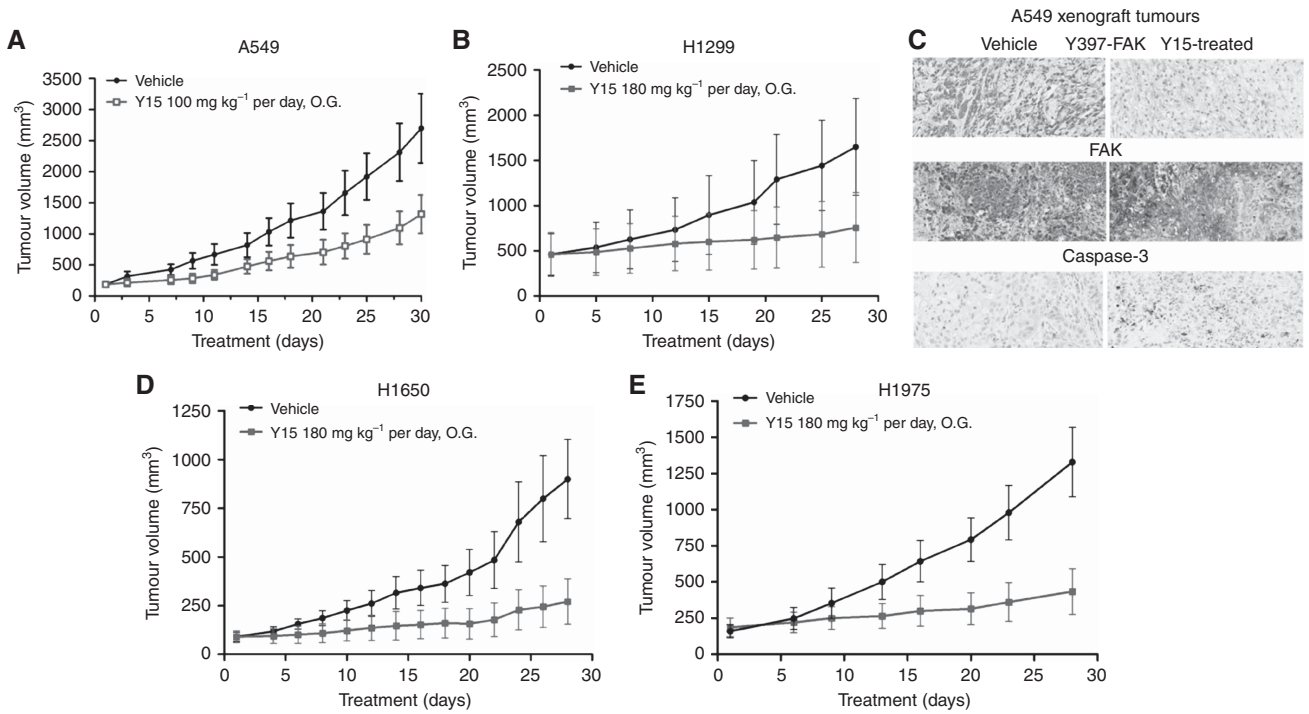

Figure 2. Y15 decreased Ras-mutant and EGFR-mutant lung cancer tumour growth *in vivo*. (**A**) KRAS-mutant cell A549 were injected subcutaneously into the flank of mice ($n=5$), and Y15 was administrated at 100 mg kg^{-1} orally by gavage 5 days a week. 1 × PBS was administered orally by gavage to untreated group. Tumour volume was measured as described in the 'Materials and Methods' section. *$P<0.05$, Student's *t*-test. (**B**) The same experiment was performed with NRAS-mutant cell H1299 xenograft tumour growth. Y15 was administrated at 180 mg kg^{-1} by gavage (based on dose–response across multiple cell lines showing that 180 mg kg^{-1} can consistently show difference in tumour growth inhibition compared with 100 mg kg^{-1} dose). (**C**) Y15 decreased Y397-pFAK in tumour xenograft tissues. Tumours from A549 xenograft were collected and used for immunohistochemical staining with Y397-pFAK, FAK and caspase-3. Y15-treated tumours expressed less Y397-pFAK than untreated tumours. Activation of caspase-3 was observed in Y15-treated tumours. (**D**, **E**) Same treatments performed with EGFR-mutant H1650 (**D**) with intrinsic resistance to EGFR TKI and H1975 cell line (**E**) with known EGFR T790M resistance mutation.

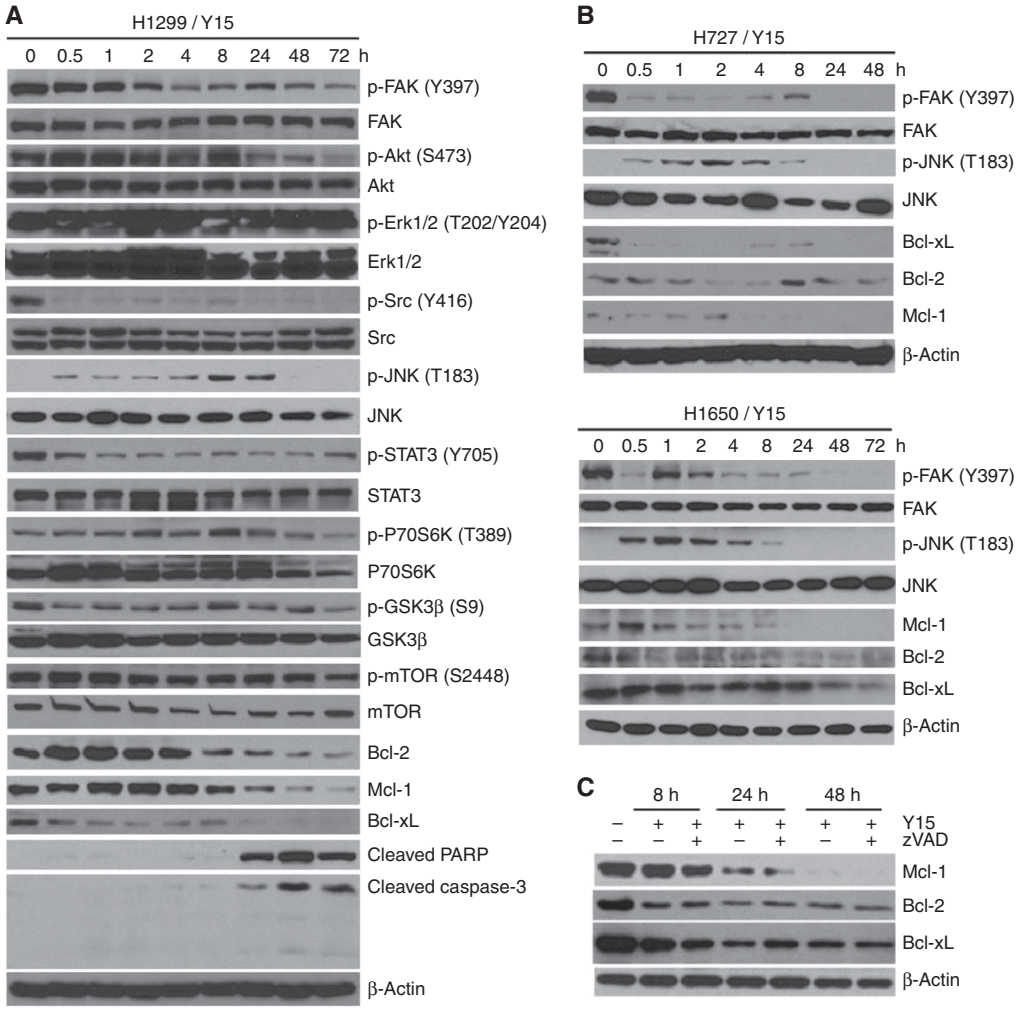

Figure 3. Y15 inhibits Y397 FAK autophosphorylation and downregulates Bcl-2 family members. (**A**) Y15 decreased Y397-pFAK and downstream p-Src, p-Akt targets in a time-dependent manner. H1299 lung cancer cell line was treated with 5 μM of Y15 for 0–72 h and western blotting was performed with Y397-pFAK, FAK, p-Src, Src, p-Akt, Akt and other targets. Y15 increased cleaved PARP and caspase-3 starting from 24 h. (**B**) Y15 performed similar effects in H727 and H1650 in a time-dependent manner. (**C**) Downregulation of Bcl-2 family members was independent of caspase activation. Twenty μM of broad-spectrum caspase inhibitor, z-VAD-fmk, was treated with or without 5 μM Y15 at different time points after 8–48 h in the H1299 cells. Western blotting was performed to evaluate the effect on Bcl-2 family members.

Activation of JNK contributes to Y15-induced downregulation of Bcl-2 family members. It was reported that JNK is involved in downregulation of Bcl-2 family members (Yamamoto *et al*, 1999; Inoshita *et al*, 2002; Basu and Haldar, 2003). To elucidate the effects of JNK activation on induction of apoptosis, knockdown of JNK by siRNA (si-JNK) was used in selected Y15-sensitive cells (H1299, H1650 and H358). As shown in Figure 4A, in the presence of 5 μM Y15 treatment alone, p-JNK (T183) was significantly activated, whereas both p-FAK (Y397) and p-Akt (S473) were inhibited in the tested cell lines. In contrast with the siRNA-negative control, the expression of JNK was totally abrogated by siRNA in H1299, H1650 and H358 si-JNK cell lines. Furthermore, the previously observed degradation of Mcl-1, Bcl-xL and Bcl-2 upon treatment with Y15 alone was substantially attenuated upon knockdown of JNK (Figure 4A). Notably, the decrease of Mcl-1 and Bcl-2 in Y15-treated si-JNK cells was minimal to absent, suggesting that JNK activation is the process upstream of Mcl-1 and Bcl-2 regulation, and exhibits a functional role in the attenuation of apoptosis in si-JNK cells. JNK downregulation by siRNA protected cells from Y15-induced cell death in H1299, H358 and H1650 cells (Figure 4B; $P<0.001$, 0.00368, <0.001, respectively. Raw data is provided in the Supplementary Materials), supporting the hypothesis that activation of JNK contributes to Y15-induced apoptosis. Together, these results demonstrate that JNK activation has an important role in Y15-induced downregulation of Bcl-2 family members.

Abrogation of anti-apoptotic Bcl-2 family proteins synergizes with inhibition of FAK in lung cancer. As there was decreased Akt phosphorylation and downregulation of both Bcl-2 and Bcl-xL upon treatment with Y15 over time, we hypothesised that targeting these proteins may modulate the efficacy of Y15. To determine the role of these proteins, we knocked down Bcl-2, Bcl-xL or Akt1 by shRNA in H1299 cells. Stable clones propagated after puromycin selection (1 μg ml^{-1}) were then treated with Y15 and the results were compared with parental H1299 cell lines using trypan blue exclusion method. Figure 5A shows that knockdown of either Bcl-2 or Bcl-xL significantly decreased cell viability upon exposure to Y15, whereas no additional effect was observed with knockdown of Akt1. Figure 5B shows the expression of Akt1, Bcl-2, Bcl-xL in infected clones *vs* control cells that express the vector alone. In contrast to treatment control cells, there was minimal or modest decrease of Mcl-1 observed in shAkt1 clones upon treatment with

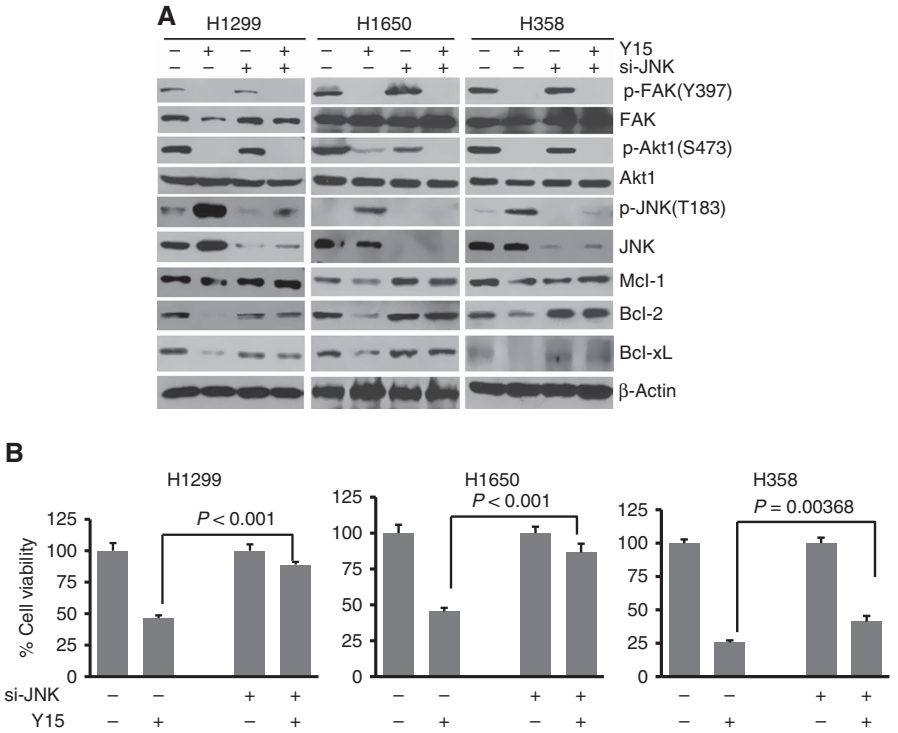

Figure 4. Knockdown of JNK by siRNA significantly attenuates Y15-induced cytotoxicity, and subsequently abrogates Mcl-1 and Bcl-2 downregulation induced by Y15. H1299, H1650 or H358 cells were transfected with siRNA targeting JNK and were treated with Y15 for 48 h, after which whole-cell lysates were prepared and subjected to western blot analysis (**A**). The extent of apoptosis was determined as described in the 'Materials and Methods' section (**B**). Twenty-four hours after siRNA transfection, cells were treated with Y15 (2.5 μM for H1299, and 5 μM for H358 and H1650) for 24 h. Then cells were collected and live cells were quantified with trypan blue exclusion methods. Results of Y15-treated cells were presented as % relative to values of vehicle-treated cells (defined as 100%). Data represents means ± s.d. of three independent experiments (*$P<0.05$, compared with scrambled siRNA control).

Y15. In comparison, Mcl-1 levels were markedly reduced in shBcl-xL and shBcl-2 clones treated with Y15.

To investigate the signalling effects with pharmacologic inhibition, the effects of the combination of Y15 and the Bcl-2/Bcl-xL inhibitor ABT263 are illustrated in Figure 5C–E. The combination of Y15 and ABT263 decreased Mcl-1 levels to a greater degree than either Y15 or ABT263 alone. This combination also abrogated Akt (S473) and STAT3 (Y705) phosphorylation to a greater degree than that can be achieved by Y15 alone (Figure 5C). Consistent with the signalling effects, cell-viability tests showed that either Y15 or ABT263 alone was minimally toxic to H1299 cells. However, exposure of cells to the combination markedly increased cell death (i.e., >72%; Figure 5D). Median dose–effect analysis yielded combination index values considerably < 1.0, corresponding to a highly synergistic interaction (Figure 5E).

MTS assay was thus subsequently performed to evaluate the effect of Y15 or other FAK inhibitors in combination with various Bcl-2 inhibitors across different lung cancer cell lines. Supplementary Table S1 summarises the results. Synergism is demonstrated with the combination of FAK inhibitors with various Bcl-2 inhibitors across multiple lung cancer cell lines.

DISCUSSION

Metastatic non-small cell lung cancer remains a difficult-to-treat disease, and efforts to improve patient survival have yielded moderate success so far even with genotypically selected targeted therapies. Emerging evidence has implicated FAK to have a key signalling role that induces cancer cell proliferation, motility, survival, invasion and metastasis (Dunn *et al*, 2010). In this study, we demonstrated that treatment with Y15 significantly decreased viability and clonogenicity of several lung cancer cell lines. Y15 is a non-receptor tyrosine kinase FAK inhibitor, which effectively decreased Y397 FAK phosphorylation in a time- and dose-dependent manner, and also decreased phosphorylation of downstream FAK signalling players, such as Src, Akt and STAT3. Downregulation of Bcl-2 family members (Bcl-2, Bcl-xL and Mcl-1) was associated with Y15-induced apoptosis. This in turn requires activation of JNK, with subsequent Mcl-1 and Bcl-2 downregulation. Y15-induced downregulation of the anti-apoptotic Bcl-2 is an important characteristic in key contradistinction to other FAK inhibitors where there is no significant effect on Bcl-2 or Bcl-xL levels (Yoon *et al*, 2014). Although Mcl-1 down-regulation was described with another FAK inhibitor (Yoon *et al*, 2014), the effect was transient, whereas this is sustained with exposure to Y15.

This is the first report to demonstrate the efficacy of FAK inhibition in H1975, an EGFR-mutant lung cancer cell line harbouring the T790M mutation resistant to first- and second-generation EGFR tyrosine kinase inhibitors (TKIs). This is an important finding as Y15 may demonstrate activity regardless of the EGFR mutation type, particularly as different EGFR mutations have varying sensitivity to currently used EGFR TKIs and drug resistance continues to be a significant clinical problem despite the development of third-generation TKIs. Moreover, we also demonstrated the efficacy of FAK inhibition in RAS-driven lung cancer, supporting observations reported previously that FAK inhibitors exert potent antitumour effects in mutant KRAS non-small cell lung cancer in association with INK4A/ARF deficiency (Konstantinidou *et al*, 2013).

Recent reports demonstrated that the anti-apoptotic PI3K/Akt cascade promotes resistance to various anti-cancer therapies,

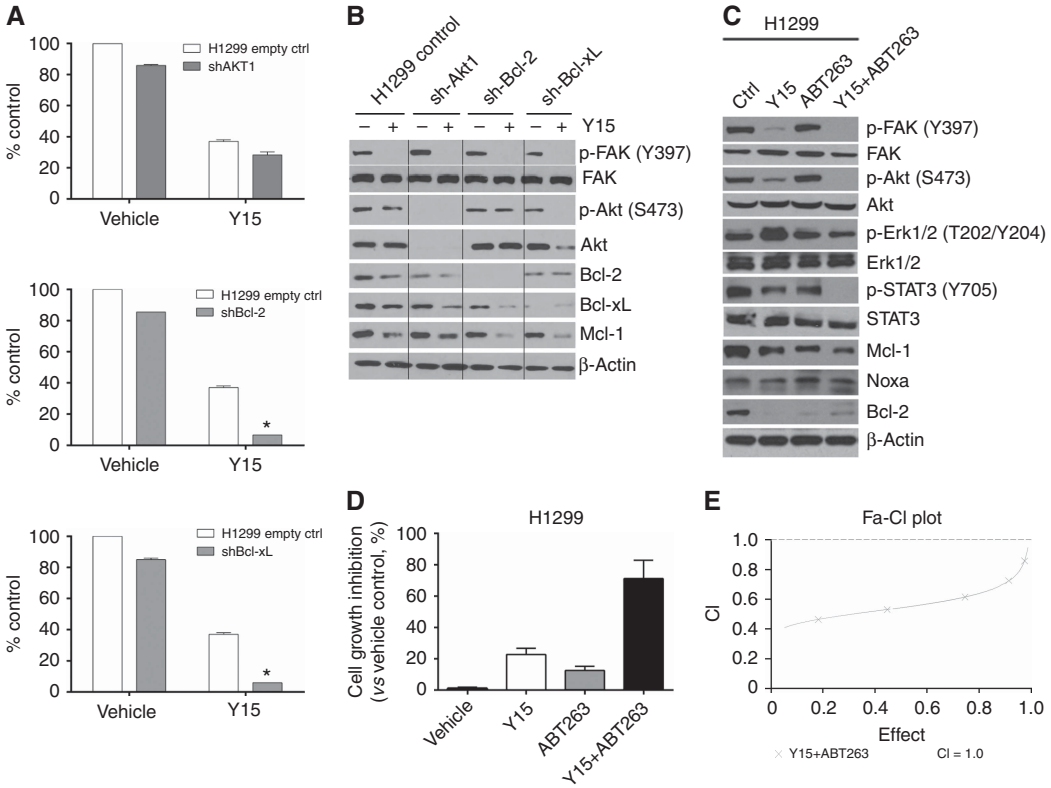

Figure 5. Abrogation of anti-apoptotic Bcl-2 family members synergizes the antitumour efficacy of Y15 against lung cancer cells *in vitro*. (**A**) H1299 cells with empty vector and their respective shBcl-2, shBcl-xL or shAkt1 clones were treated with Y15 for 72 h, trypan blue assay was performed to evaluate cell viability. (**B**) Western blots showing differences in the expression of Bcl-2, Bcl-xL and Akt1 in control H1299 and respective shRNA clone cells, with or without Y15. (**C**) Western blot showing the effect on downstream signalling proteins with the combination of Y15 at 5 μM and the Bcl-2/Bcl-xL inhibitor ABT263 at 2.5 μM in H1299 cells after 24 h treatment. The combination of Y15 and ABT263 decreased Y397-pFAK, p-Src and p-Akt more than each agent alone. (**D**) ABT263 potentiates Y15-mediated apoptosis. The cell growth inhibition was determined as described in the 'Materials and Methods' section. Data represent means ± s.d. of three independent experiments. (**E**) Median dose–effect analysis was performed to calculate CI using CalcuSyn software (Biosoft) to determine interactions of Y15 combined with ABT263.

including EGFR TKIs (Tsuruta *et al*, 2002; Konstantinidou *et al*, 2009; Jeannot *et al*, 2014).The Bcl-2 family also represents a critical group of molecules involved directly in the regulation of cell apoptosis (Reynolds *et al*, 1994; Adams and Cory, 1998; Reed, 1998; Gross *et al*, 1999). Indeed, the lack of efficacy of combined PI3K/Akt and MEK pathway inhibition in KRAS-mutant lung cancers can be attributed to the inability to induce apoptosis, as inhibition of Bcl-xL restores cytotoxicity and the apoptotic response (Hata *et al*, 2014). We have demonstrated that Y15 induces apoptosis. Our results showed that Bcl-2, Bcl-xL and Mcl-1 downregulation contributed significantly to Y15-induced apoptosis. In addition, combination therapy with Bcl-2/Bcl-xL inhibitor, such as ABT263, potentiates Y15-mediated apoptosis (Figure 5D and E). Similar to what has been recently demonstrated in ovarian clear cell carcinoma cell lines (Yoon *et al*, 2014), we also demonstrated that pharmacological inhibition of Bcl-2/Bcl-xL in combination with various FAK inhibitors including Y15 has synergistic activity in lung cancer cell lines. One potential mechanism for the synergistic effect between Bcl-2 pathway inhibition with kinase inhibitors had been demonstrated previously by multiple groups of investigators (Costa *et al*, 2007; Gong *et al*, 2007; Ng *et al*, 2012; Tanizaki *et al*, 2012; Tan *et al*, 2013; Zaanan *et al*, 2015). These studies demonstrate that upregulation of BIM, a pro-apoptotic member of the Bcl-2 family, improves that apoptotic effect induced by various kinase inhibitors across different malignancies, including MAPK pathway-activated cancers, such as RAS-mutant or EGFR-mutant in lung cancer. Conversely, polymorphic variants that lead to BIM isoforms lacking the pro-apoptotic BH3 domain may underlie innate primary resistance to therapy. Drugs such as ABT263 sequester Bcl-2 and Bcl-xL to release BIM, thereby enhancing the efficacy of kinase inhibitors. Moreover, paxillin, an adaptor protein that is phosphorylated by FAK and Src, is shown to confer resistance to EGFR TKIs in EGFR-mutant lung cancers by reducing BIM and increasing Mcl-1 expression (Wu *et al*, 2015). Finally, inactivation of STAT3 by Y15 contributes to reduction in Bcl-xL expression, thereby enhancing the apoptotic potential of the combination regimen (Zhang *et al*, 2012; Zaanan *et al*, 2015).

We conducted experiments to describe another mechanism of the synergism observed between FAK inhibition and Bcl-2 pathway inhibition. JNK is a member of the MAPK family and is activated by a variety of environmental stresses, inflammatory cytokines, growth factors and GPCR agonists (Bogoyevitch *et al*, 2010). Recent studies demonstrated that JNK is involved in down-regulation of Bcl-2 family members (Yamamoto *et al*, 1999; Inoshita *et al*, 2002; Basu and Haldar, 2003). In our study, JNK activation has a role in Y15-induced downregulation of Mcl-1 and Bcl-2. Knockdown of JNK by shRNA abrogated the down-regulation of Mcl-1 and Bcl-2 by Y15 and attenuated Y15-induced cell lethality, indicating that JNK activation is the upstream process of Mcl-1 and Bcl-2 regulation. Altering JNK function or activity may thus affect the efficacy of Y15, or potentially, as well as on the combination of FAK and Bcl-2/Bcl-xL inhibitors.

In summary, this report for the first time demonstrates the effect of FAK inhibition alone or in combination with depletion of Bcl-2 pathway in oncogenically driven, MAPK-activated lung cancers

through either RAS or EGFR mutation. FAK signalling is a novel therapeutic target worth exploring in the treatment of lung cancer, and the data shown here provide the rationale for further clinical development.

ACKNOWLEDGEMENTS

Major funding for this project was received from RPCI Alliance Foundation. This work was also made possible in part by National Institute of Health Grant, CA65910 and P30 Grant CA016056 from NCI to Roswell Park Cancer Institute. We also thank the Support in part by the Fundamental Research Funds for the Central Universities, Shaanxi Normal University (GK201603062). We thank Mike Yemma and Baotran Ho for their assistance with the harvest of A549 xenograft experiments for histopathological analysis.

CONFLICT OF INTEREST

The authors declare no conflict of interest.

REFERENCES

Adams J, Cory S (1998) The Bcl-2 protein family: arbiters of cell survival. *Science* **281**: 1322–1326.

Agochiya M, Brunton VG, Owens DW, Parkinson EK, Paraskeva C, Keith WN, Frame MC (1999) Increased dosage and amplification of the focal adhesion kinase gene in human cancer cells. *Oncogene* **18**: 5646–5653.

Bailey KM, Liu J (2008) Caveolin-1 up-regulation during epithelial to mesenchymal transition is mediated by focal adhesion kinase. *J Biol Chem* **283**: 13714–13724.

Basu A, Haldar S (2003) Identification of a novel Bcl-xL phosphorylation site regulating the sensitivity of taxol-or 2-methoxyestradiol-induced apoptosis. *FEBS Lett* **538**: 41–47.

Beierle EA, Ma X, Stewart J, Nyberg C, Trujillo A, Cance WG, Golubovskaya VM (2010) Inhibition of focal adhesion kinase decreases tumor growth in human neuroblastoma. *Cell Cycle* **9**: 1005–1015.

Bogoyevitch MA, Ngoei KR, Zhao TT, Yeap YY, Ng DC (2010) c-Jun N-terminal kinase (JNK) signaling: recent advances and challenges. *Proteins Proteomics* **1804**: 463–475.

Carelli S, Zadra G, Vaira V, Falleni M, Bottiglieri L, Nosotti M, Di Giulio AM, Gorio A, Bosari S (2006) Up-regulation of focal adhesion kinase in non-small cell lung cancer. *Lung Cancer* **53**: 263–271.

Carretero J, Shimamura T, Rikova K, Jackson AL, Wilkerson MD, Borgman CL, Buttarazzi MS, Sanofsky BA, McNamara KL, Brandstetter KA (2010) Integrative genomic and proteomic analyses identify targets for Lkb1-deficient metastatic lung tumors. *Cancer Cell* **17**: 547–559.

Cary LA, Chang JF, Guan JL (1996) Stimulation of cell migration by overexpression of focal adhesion kinase and its association with Src and Fyn. *J Cell Sci* **109**: 1787–1794.

Chen Z, Cheng K, Walton Z, Wang Y, Ebi H, Shimamura T, Liu Y, Tupper T, Ouyang J, Li J (2012) A murine lung cancer co-clinical trial identifies genetic modifiers of therapeutic response. *Nature* **483**: 613–617.

Cicchini C, Laudadio I, Citarella F, Corazzari M, Steindler C, Conigliaro A, Fantoni A, Amicone L, Tripodi M (2008) TGFbeta-induced EMT requires focal adhesion kinase (FAK) signaling. *Exp Cell Res* **314**: 143–152.

Costa DB, Halmos B, Kumar A, Schumer ST, Huberman MS, Boggon TJ, Tenen DG, Kobayashi S (2007) BIM mediates EGFR tyrosine kinase inhibitor-induced apoptosis in lung cancers with oncogenic EGFR mutations. *PLoS Med* **4**: e315.

Dunn KB, Heffler M, Golubovskaya V (2010) Evolving therapies and FAK inhibitors for the treatment of cancer. *Anticancer Agents Med Chem* **10**: 722–734.

Golubovskaya VM, Nyberg C, Zheng M, Kweh F, Magis A, Ostrov D, Cance WG (2008) A small molecule inhibitor, 1,2,4,5-benzenetetraamine tetrahydrochloride, targeting the y397 site of focal adhesion kinase decreases tumor growth. *J Med Chem* **51**: 7405–7416.

Gong Y, Somwar R, Politi K, Balak M, Chmielecki J, Jiang X, Pao W (2007) Induction of BIM is essential for apoptosis triggered by EGFR kinase inhibitors in mutant EGFR-dependent lung adenocarcinomas. *PLoS Med* **4**: e294.

Gross A, McDonnell J, Korsmeyer S (1999) Bcl-2 family members and the mitochondria in apoptosis. *Genes Dev* **13**: 1899–1911.

Hata AN, Yeo A, Faber AC, Lifshits E, Chen Z, Cheng KA, Walton Z, Sarosiek KA, Letai A, Heist RS (2014) Failure to induce apoptosis via BCL-2 family proteins underlies lack of efficacy of combined MEK and PI3K inhibitors for KRAS-mutant lung cancers. *Cancer Res* **74**: 3146–3156.

Heffler M, Golubovskaya VM, Cance WG, Bullar Dunn KM (2011) A small molecule FAK inhibitor increases the cytotoxicity of 5-fluorouracil. *Mol Cancer Ther* **10**: C184.

Heffler M, Zhao Y, Cance WG, Golubovskaya V, Bullar Dunn K (2010) The effect of a novel small molecule inhibitor of FAK on viability of human colon cancer cells. *J Clin Oncol* **28**: e13635.

Hochwald SN, Nyberg C, Zheng M, Zheng D, Wood C, Massoll NA, Magis A, Ostrov D, Cance WG, Golubovskaya VM (2009) A novel small molecule inhibitor of FAK decreases growth of human pancreatic cancer. *Cell Cycle* **8**: 2435–2443.

Inoshita S, Takeda K, Hatai T, Terada Y, Sano M, Hata J, Umezawa A, Ichijo H (2002) Phosphorylation and inactivation of myeloid cell leukemia 1 by JNK in response to oxidative stress. *J Biol Chem* **277**: 43730–43734.

Jeannot V, Busser B, Brambilla E, Wislez M, Robin B, Cadranel J, Coll JL, Hurbin A (2014) The PI3K/AKT pathway promotes gefitinib resistance in mutant KRAS lung adenocarcinoma by a deacetylase-dependent mechanism. *Int J Cancer* **134**: 2560–2571.

Konstantinidou G, Bey EA, Rabellino A, Schuster K, Maira MS, Gazdar AF, Amici A, Boothman DA, Scaglioni PP (2009) Dual phosphoinositide 3-kinase/mammalian target of rapamycin blockade is an effective radiosensitizing strategy for the treatment of non–small cell lung cancer harboring K-RAS mutations. *Cancer Res* **69**: 7644–7652.

Konstantinidou G, Ramadori G, Torti F, Kangasniemi K, Ramirez RE, Cai Y, Behrens C, Dellinger MT, Brekken RA, Wistuba II (2013) RHOA-FAK is a required signaling axis for the maintenance of KRAS-driven lung adenocarcinomas. *Cancer Discov* **3**: 444–457.

Kurenova EV, Hunt DL, He D, Magis AT, Ostrov DA, Cance WG (2009) Small molecule chloropyramine hydrochloride (C4) targets the binding site of focal adhesion kinase and vascular endothelial growth factor receptor 3 and suppresses breast cancer growth *in vivo*. *J Med Chem* **52**: 4716–4724.

Lazebnik Y (2010) What are the hallmarks of cancer? *Nat Rev Cancer* **10**: 232–233.

Mitra SK, Hanson DA, Schlaepfer DD (2005) Focal adhesion kinase: in command and control of cell motility. *Nat Rev Mol Cell Biol* **6**: 56–68.

Ng KP, Hillmer AM, Chuah CT, Juan WC, Ko TK, Teo AS, Ariyaratne PN, Takahashi N, Sawada K, Fei Y (2012) A common BIM deletion polymorphism mediates intrinsic resistance and inferior responses to tyrosine kinase inhibitors in cancer. *Nat Med* **18**: 521–528.

Reed J (1998) Bcl-2 family proteins. *Oncogene* **17**: 3225–3236.

Reynolds J, Yang T, Qian L, Jenkinson J, Zhou P, Eastman A, Craig R (1994) Mcl-1, a member of the Bcl-2 family, delays apoptosis induced by c-Myc overexpression in Chinese hamster ovary cells. *Cancer Res* **54**: 6348–6352.

Schlaepfer DD, Hanks SK, Hunter T, van der Geer P (1994) Integrin-mediated signal transduction linked to Ras pathway by GRB2 binding to focal adhesion kinase. *Nature* **372**: 786–791.

Shao H, Gao C, Tang H, Zhang H, Roberts LR, Hylander BL, Repasky EA, Ma WW, Qiu J, Adjei AA (2012) Dual targeting of mTORC1/C2 complexes enhances histone deacetylase inhibitor-mediated anti-tumor efficacy in primary HCC cancer *in vitro* and *in vivo*. *J Hepatol* **56**: 176–183.

Siesser PM, Hanks SK (2006) The signaling and biological implications of FAK overexpression in cancer. *Clin Cancer Res* **12**: 3233–3237.

Tan N, Wong M, Nannini MA, Hong R, Lee LB, Price S, Williams K, Savy PP, Yue P, Sampath D (2013) Bcl-2/Bcl-xL inhibition increases the efficacy of MEK inhibition alone and in combination with PI3 kinase inhibition in lung and pancreatic tumor models. *Mol Cancer Ther* **12**: 853–864.

Tanizaki J, Okamoto I, Takezawa K, Sakai K, Azuma K, Kuwata K, Yamaguchi H, Hatashita E, Nishio K, Janne P (2012) Combined effect

of ALK and MEK inhibitors in EML4–ALK-positive non-small-cell lung cancer cells. *Br J Cancer* **106**: 763–767.

Tsuruta F, Masuyama N, Gotoh Y (2002) The phosphatidylinositol 3-kinase (PI3K)-Akt pathway suppresses Bax translocation to mitochondria. *J Biol Chem* **277**: 14040–14047.

Wu D, Chen C, Chu C, Lee H (2015) Paxillin confers resistance to tyrosine kinase inhibitors in EGFR-mutant lung cancers via modulating BIM and Mcl-1 protein stability. *Oncogene* **35**: 621–630.

Yamamoto K, Ichijo H, Korsmeyer SJ (1999) BCL-2 is phosphorylated and inactivated by an ASK1/Jun N-terminal protein kinase pathway normally activated at G2/M. *Mol Cell Biol* **19**: 8469–8478.

Yoon H, Choi Y-L, Song J-Y, Do I, Kang SY, Ko Y-H, Song S, Kim B-G (2014) Targeted Inhibition of FAK, PYK2 and BCL-XL synergistically enhances apoptosis in ovarian clear cell carcinoma cell lines. *PloS ONE* **9**: e88587.

Zaanan A, Okamoto K, Kawakami H, Khazaie K, Huang S, Sinicrope FA (2015) The mutant KRAS gene up-regulates BCL-XL protein via STAT3 to confer apoptosis resistance that is reversed by BIM protein induction and BCL-XL antagonism. *J Biol Chem* **290**: 23838–23849.

Zhang H, Hylander B, Levea C, Repasky E, Straubinger R, Adjei A, Ma W (2014) Enhanced FGFR signalling predisposes pancreatic cancer to the effect of a potent FGFR inhibitor in preclinical models. *Br J Cancer* **110**: 320–329.

Zhang X, Yue P, Page BD, Li T, Zhao W, Namanja AT, Paladino D, Zhao J, Chen Y, Gunning PT (2012) Orally bioavailable small-molecule inhibitor of transcription factor Stat3 regresses human breast and lung cancer xenografts. *Proc Natl Acad Sci* **109**: 9623–9628.

Supplementary Information accompanies this paper on British Journal of Cancer website (http://www.nature.com/bjc)